Dipole-Dipole Frequency Shifts in Multilevel Atoms

A. Cidrim,[1,2,3] A. Piñeiro Orioli,[2,3] C. Sanner,[2] R. B. Hutson,[2] J. Ye,[2] R. Bachelard,[1] and A. M. Rey[2,3]
[1]Departamento de Física, Universidade Federal de São Carlos, 13565-905 São Carlos, São Paulo, Brazil
[2]JILA, NIST, Department of Physics, University of Colorado, Boulder, Colorado 80309, USA
[3]Center for Theory of Quantum Matter, University of Colorado, Boulder, Colorado 80309, USA

(Received 11 February 2021; revised 25 April 2021; accepted 19 May 2021; published 30 June 2021)

Dipole-dipole interactions lead to frequency shifts that are expected to limit the performance of next-generation atomic clocks. In this work, we compute dipolar frequency shifts accounting for the intrinsic atomic multilevel structure in standard Ramsey spectroscopy. When interrogating the transitions featuring the smallest Clebsch-Gordan coefficients, we find that a simplified two-level treatment becomes inappropriate, even in the presence of large Zeeman shifts. For these cases, we show a net suppression of dipolar frequency shifts and the emergence of dominant nonclassical effects for experimentally relevant parameters. Our findings are pertinent to current generations of optical lattice and optical tweezer clocks, opening a way to further increase their current accuracy, and thus their potential to probe fundamental and many-body physics.

DOI: 10.1103/PhysRevLett.127.013401

Introduction.—Current optical atomic clocks have reached unprecedented precision and accuracy [1–10], making them cutting-edge platforms for many technological applications and for the exploration of many-body [11–20] and fundamental physics [21–25]. The reduction of noise in atomic detection and laser stabilization in such systems has allowed measurements of the atomic transition with submillihertz resolution [6,26,27]. At this point, dipole-dipole interactions between the atoms are expected to play an important role, in the form of induced density-dependent shifts in the measured atomic transition frequency. Simple two-level models have been applied to quantitatively determine these dipolar shifts [28–34], but, in reality, atoms have a complex internal multilevel structure which has to be taken into account. This calls for a deeper understanding of the role of multiple internal levels in dipolar systems [35–39], which is also relevant for applications in quantum simulators [11,17,18,40] and quantum computing [41–43].

In this work, we investigate dipolar frequency shifts experienced by arrays of multilevel atoms in a Ramsey spectroscopy protocol. In general, the strength of dipolar interactions is set by the magnitude of the transition's dipole moment, which is proportional to a Clebsch-Gordan coefficient (CGC). However, in multilevel atoms the dependence of the dipolar shift on the choice of transition is more complex. This is because the CGC between two specific states not only sets the strength of the dipole couplings, but also affects the coupling strength to nearby levels. Specifically, transitions with low (high) CGC feature a stronger (weaker) decay to and interactions with their neighboring states.

Our results show that the magnitude of the dipolar frequency shift is mainly controlled by the CGC of the *interrogated* levels. Therefore, one can strongly suppress dipolar shifts by selectively choosing the levels with the smallest CGC. We also find that interactions with nearby levels can significantly modify the shift. Specifically, we show that a full multilevel calculation is necessary when the CGC of the interrogated transition is small, whereas simplified two-level models are accurate when the CGC is large. Surprisingly, the relevance of the multilevel structure holds even in the presence of strong magnetic fields, under which the large Zeeman shifts suppress exchange with nearby levels. Moreover, we find that the suppression of the shift from small CGC leads to an increased relative importance of beyond-mean-field effects for specific experimentally relevant array geometries and laser wave vector configurations. In short, our work offers a simple way for current experiments to reduce dipolar shifts by almost 2 orders of magnitude, while at the same time drawing theorists' attention to the important yet largely neglected role of internal levels in many-body dipolar systems.

Multilevel coupled dipole model.—We consider a system of N pointlike atoms pinned in a deep optical lattice or a tweezer array with unity occupation, always in their motional ground state. We assume that each atom i has a multilevel internal structure of ground and excited manifolds, g and e, with respective total angular momenta F_g and F_e. There are thus $(2F_a+1)$ hyperfine states $|a_m\rangle_i \equiv |a, F_a, m\rangle_i$ with angular momentum projections $m \in [-F_a, F_a]$, for each manifold $a \in \{g, e\}$. The photon-mediated interaction between the atoms occurs via both coherent exchange and incoherent decay of excitations [see

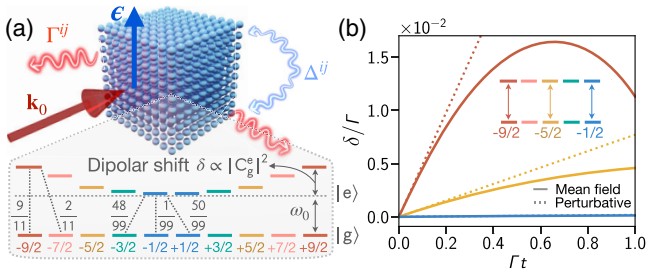

FIG. 1. (a) Ramsey spectroscopy for multilevel atoms with internal level structure $F_g = F_e = 9/2$ in an optical lattice. The atoms are prepared in a superposition of a particular ground and excited pair of states g_α and e_β by a laser with wave vector $\mathbf{k}_0$, polarization ϵ, and pulse area θ. During a dark time t, the atoms interact via coherent and incoherent dipole-dipole processes, Δ^{ij} and Γ^{ij}, respectively. This induces a frequency shift $\delta^{g_\alpha e_\beta} \sim |C^{e_\beta}_{g_\alpha}|^2$ controlled by the CGC of the interrogated transition. The schematic form of the dipolar shift corresponding to interrogating π-polarized transitions (colored according to their CGC) is depicted here. CGCs squared for different $\sigma^\pm$ and π transitions are displayed. (b) Shift from the Ramsey protocol addressing three different π-polarized transitions for a 3D lattice of spacing $d = 7\lambda/12$ with $N = 10^3$ atoms and $\theta = \pi/2$.

Fig. 1(a)], and the dipole dynamics can be modeled by a *multilevel coupled dipole master equation* [38,39,44–46] $\dot{\hat{\rho}} = -i[\hat{H}, \hat{\rho}(t)] + \mathcal{L}(\hat{\rho})$ ($\hbar = 1$), where

$$\hat{H} = -\sum_{i,j} \Delta^{ij}_{g_m e_n, g_{m'} e_{n'}} \hat{\sigma}^{e_n g_m}_i \hat{\sigma}^{g_{m'} e_{n'}}_j, \tag{1}$$

$$\mathcal{L}(\hat{\rho}) = \sum_{i,j} \Gamma^{ij}_{g_m e_n, g_{m'} e_{n'}} (2\hat{\sigma}^{g_{m'} e_{n'}}_j \hat{\rho} \hat{\sigma}^{e_n g_m}_i - \{\hat{\sigma}^{e_n g_m}_i \hat{\sigma}^{g_{m'} e_{n'}}_j, \hat{\rho}\}), \tag{2}$$

and $\hat{\sigma}^{a_m b_n}_i = |a_m\rangle_i \langle b_n|_i$. For a two-level atom, these operators become the usual raising/lowering Pauli operators. For clarity, we have used Einstein notation for levels in the equations above (i.e., repeated indices m, m', n, or n' are summed). The terms proportional to $\Delta^{ij}_{g_m e_n, g_{m'} e_{n'}}$ and $\Gamma^{ij}_{g_m e_n, g_{m'} e_{n'}}$ characterize the elastic and dissipative components of the dipolar interactions and their amplitudes relate to the free-space electromagnetic Green's tensor $\mathbf{G}_{ij} \equiv \mathbf{G}(\mathbf{r}_i - \mathbf{r}_j)$ of an oscillating point dipole at position $\mathbf{r}_j$ according to

$$\begin{aligned} \Delta^{ij}_{g_m e_n, g_{m'} e_{n'}} &\equiv C^{e_n}_{g_m} \mathbf{e}^*_{n-m} \cdot \mathrm{Re}\{\mathbf{G}_{ij}\} \cdot C^{e_{n'}}_{g_{m'}} \mathbf{e}_{n'-m'}, \\ \Gamma^{ij}_{g_m e_n, g_{m'} e_{n'}} &\equiv C^{e_n}_{g_m} \mathbf{e}^*_{n-m} \cdot \mathrm{Im}\{\mathbf{G}_{ij}\} \cdot C^{e_{n'}}_{g_{m'}} \mathbf{e}_{n'-m'}, \end{aligned} \tag{3}$$

where $C^{e_n}_{g_m} \equiv \langle F_g, m; 1, n-m | F_e, n\rangle$ is the CGC of the transition $g_m \leftrightarrow e_n$ with polarization vector $\mathbf{e}_{n-m}$. We define the spherical basis $\mathbf{e}_0 = \hat{z}$, $\mathbf{e}_{\pm 1} = \mp(\hat{x} \pm i\hat{y})/\sqrt{2}$. The vacuum Green's tensor is given by $\mathbf{G}(\mathbf{r}) = (3\Gamma/4)(e^{ik_0 r}/(k_0 r)^3)[(k_0^2 r^2 + ik_0 r - 1)\mathbb{1} - (k_0^2 r^2 + i3k_0 r - 3)\hat{\mathbf{r}} \otimes \hat{\mathbf{r}}]$, where $\hat{\mathbf{r}} = \mathbf{r}/r$, $r = |\mathbf{r}|$. $\Gamma = |d_{eg}|^2 k_0^3/[3\pi\hbar\epsilon_0(2F_e + 1)]$ is the total spontaneous decay rate, d_{eg} the radial dipole matrix element, $k_0 = \omega_0/c = 2\pi/\lambda$ the atomic transition wave number and ϵ_0 the vacuum permittivity. For $i = j$, the coherent interaction coefficient is $\Delta^{ii}_{g_m e_n, g_{m'} e_{n'}} = 0$ and the incoherent term reduces to the single-particle spontaneous decay term $\Gamma^{ii}_{g_m e_n, g_{m'} e_{n'}} = \delta_{n-m, n'-m'} C^{e_n}_{g_m} C^{e_{n'}}_{g_{m'}} \Gamma/2$. Note that the total decay rate $\Gamma_{e_n} \equiv 2\sum_m \Gamma^{ii}_{g_m e_n, g_m e_n} = \Gamma$ is the same for any excited state e_n because of the sum rule $\sum_m |C^{e_n}_{g_m}|^2 = 1$.

Ramsey spectroscopy with multilevel atoms.—We investigate the effect of the atomic multilevel nature on the following Ramsey spectroscopy protocol assuming, at first, zero external magnetic field. We start by selecting a pair of states g_α and e_β, driving the transition between them with a resonant laser of pulse area θ, wave vector $\mathbf{k}_0$, and polarization $\boldsymbol{\epsilon}$. The laser drive is assumed to be much stronger than the interaction energies, such that it creates an uncorrelated coherent superposition $|\Psi_{g_\alpha, e_\beta}\rangle = \otimes_j [\cos(\theta/2)|g_\alpha\rangle_j + e^{i\mathbf{k}_0 \cdot \mathbf{r}_j} \sin(\theta/2)|e_\beta\rangle_j]$. We hereafter consider $\theta = \pi/2$, as generally used in clock experiments, or $\theta = \pi/4$, as the latter can lead to more pronounced and thus easily observable dipolar shifts. Then, the system evolves freely for a dark time t. By analogy with two-level systems, we define $\langle \hat{S}^y \rangle \equiv \mathrm{Im}\{\langle \hat{S}^{e_\beta g_\alpha} \rangle\}$ and $\langle \hat{S}^x \rangle \equiv \mathrm{Re}\{\langle \hat{S}^{e_\beta g_\alpha} \rangle\}$, where the multilevel collective spin operator (under the appropriate gauge transformation that removes the phase $\mathbf{k}_0 \cdot \mathbf{r}_j$ imprinted by the laser on atom j) reads $\hat{S}^{e_\beta g_\alpha} = \sum_j e^{i\mathbf{k}_0 \cdot \mathbf{r}_j} \hat{\sigma}^{e_\beta g_\alpha}_j$. The collective vector precesses around the z direction of the Bloch sphere and accumulates an azimuthal phase as a result of the dipole-dipole interactions. The corresponding time-dependent frequency shift is defined as

$$\delta^{g_\alpha e_\beta}(t) \equiv \frac{1}{2\pi t} \arctan \frac{\langle \hat{S}^y \rangle(t)}{\langle \hat{S}^x \rangle(t)}. \tag{4}$$

Dipolar interactions also lead to a reduction of the contrast $\mathcal{C}^{g_\alpha e_\beta}(t) \equiv (1/N)\sqrt{\langle \hat{S}^x \rangle^2(t) + \langle \hat{S}^y \rangle^2(t)}$.

We employ three different types of approximations to investigate this multilevel many-body system: (i) A short-time perturbative expansion, valid for $t \ll \Gamma^{-1}$ that we use to compute the dipolar frequency shift at first order in time, i.e., $\delta^{g_\alpha e_\beta}(t) \approx \delta^{g_\alpha e_\beta}_0 + \delta^{g_\alpha e_\beta}_1 t$. (ii) A mean-field (MF) approximation, which neglects quantum correlations, i.e., $\langle \hat{\sigma}^{ab}_i \hat{\sigma}^{cd}_{j \neq i} \rangle \approx \langle \hat{\sigma}^{ab}_i \rangle \langle \hat{\sigma}^{cd}_{j \neq i} \rangle$. (iii) A second-order cumulant expansion, which factorizes three-point (and higher-order) correlations in terms of one- and two-point functions [47]. In the MF and cumulant simulations we further assume that only g_α, e_β, and their adjacent levels (i.e., $g_{\alpha \pm 1}$ and $e_{\beta \pm 1}$) play a relevant role in the dynamics, as demonstrated in [47].

Short-time perturbative expansion.—To gain physical intuition of the problem, we analytically derive short-time expressions for the shift. The zero-order shift reads

$$\delta_0^{g_\alpha e_\beta} = -\frac{\cos\theta}{2\pi N}\sum_{i,j\neq i} U^{ji}_{g_\alpha e_\beta}, \tag{5}$$

where we have defined $U^{ji}_{g_\alpha e_\beta} \equiv \Gamma^{ji}_{g_\alpha e_\beta, g_\alpha e_\beta}\sin(\mathbf{k}_0\cdot\mathbf{r}_{ij}) + \Delta^{ji}_{g_\alpha e_\beta, g_\alpha e_\beta}\cos(\mathbf{k}_0\cdot\mathbf{r}_{ij})$. Physically, the term $U^{ji}_{g_\alpha e_\beta}$ describes the classical interaction energy between two oscillating dipoles at positions $\mathbf{r}_i$ and $\mathbf{r}_j$ [28], where both coherent and incoherent processes contribute. At this order, only the transition between g_α and e_β, directly driven by the pulse, is involved and the MF treatment is exact. Furthermore, $\delta_0^{g_\alpha e_\beta}$ is proportional to $|C^{e_\beta}_{g_\alpha}|^2$ [see Eq. (3)], so that the multilevel system differs from two-level atoms [28] via a renormalization by the CGC. Note that the zero-order shift vanishes for a $\theta = \pi/2$ pulse, as the dipole-dipole induced precession of the collective Bloch vector requires a nonzero $\langle\hat{S}^z\rangle$ component.

The next-order correction does involve other levels and is given by

$$\delta_1^{g_\alpha e_\beta} = -\frac{1}{2\pi N}\sum_{i,j\neq i}\Bigg\{U^{ji}_{g_\alpha e_\beta}\tilde{\Gamma}_{g_\alpha e_\beta}(\theta) + \sum_p\Bigg(\sum_{k\neq i,j} W_p^{kji}(\theta) + \sum_{p'} Q^{ji}_{p,p'}(\theta)\Bigg)\Bigg\}, \tag{6}$$

with p and p' referring to polarizations [47].

The first contribution in Eq. (6) is similar to the zero-order shift. The $\cos\theta$, however, is replaced by $\tilde{\Gamma}_{g_\alpha e_\beta}(\theta)$, which contains a collective contribution and an explicit dependence on the CGC of the transition interrogated. The $W_p^{kji}(\theta)$ are two-photon coherent and incoherent processes between three different atoms, where one of the contributing transitions is always $g_\alpha \leftrightarrow e_\beta$. Thus, these terms are proportional to at least $|C^{e_\beta}_{g_\alpha}|^2$. The $Q^{ji}_{p,p'}(\theta)$ terms correspond to processes involving two atoms only, yet not necessarily from the $g_\alpha \leftrightarrow e_\beta$ transition. As two-photon processes, they nevertheless contain the product of four CGCs and, as we shall discuss later, they carry beyond-mean-field contributions.

Suppression of the frequency shift.—Although our conclusions are valid for generic multilevel systems, in this work we focus our analysis on the case of ^{87}Sr, given its metrological relevance for atomic clocks [1,5,11,17]. More specifically, we assume multilevel atoms with $F_g = F_e = 9/2$, organized in a 2D or 3D array with magic-wavelength spacing $d = 7\lambda/12$ [48], see Fig. 1(a). For simplicity, we will hereafter consider addressing π-polarized transitions (i.e., $\alpha = \beta$), where the quantization axis is defined by the laser polarization $\boldsymbol{\epsilon}$. For this system

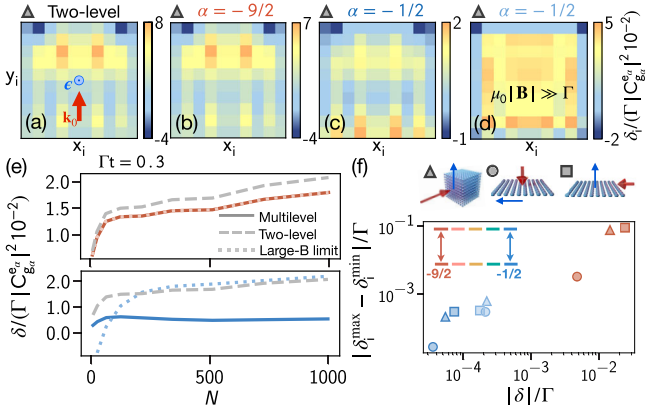

FIG. 2. Local frequency shifts δ_i for a 3D lattice with $N = 10^3$ atoms, interrogated by a laser with a pulse area of $\pi/2$ and a dark time of $\Gamma t = 0.3$ as shown in the configuration labeled by a triangle for (a) a two-level system and transitions (b) $g_{-9/2} \leftrightarrow e_{-9/2}$, (c) $g_{-1/2} \leftrightarrow e_{-1/2}$, and (d) $g_{-1/2} \leftrightarrow e_{-1/2}$ in the presence of a large magnetic field $\mathbf{B}$. The shift is calculated using Eq. (6) and is averaged along $\boldsymbol{\epsilon}$, with the resulting contribution at positions (x_i, y_i). Shifts are rescaled by the corresponding CGC squared and by an overall 10^{-2} factor. (e) Comparing the global shift of the multilevel model for transitions $\alpha = -9/2$ (top) and $\alpha = -1/2$ (bottom) (full and dotted lines, for zero and large magnetic fields, respectively) to a two-level model (dashed lines). (f) Absolute value of the difference between maximum and minimum of the local shift ($\delta_i^{\max}$ and $\delta_i^{\min}$) versus magnitude of the global shift $|\delta|$ for different geometries with $N \sim 10^3$. Symbols represent configurations shown in the legend. The light-blue symbols correspond to the large-$|\mathbf{B}|$ limit for $\alpha = -1/2$.

it is important to know that the CGC for π-polarized transitions scales as $C^{e_m}_{g_m} \propto m$, i.e., it is largest for $\pm 9/2$ and smallest for $\pm 1/2$.

A direct consequence of the zero- and first-order terms' dependence on the CGC is that the shift can be strongly suppressed by choosing the appropriate transition, i.e., the one with the lowest CGC. This effect is illustrated in Fig. 1(b), where the dark-time evolution of the shift in a 3D array is monitored for three different transitions, $\alpha = -9/2$, $-5/2$, and $-1/2$. As a consequence of the scaling with the CGC, the shift is reduced by a factor 81 for the $\alpha = -1/2$ transition, as compared to $\alpha = -9/2$. Note that the suppression remains valid even at longer times beyond the regime of validity of the short-time expansion. The decay of the contrast $\mathcal{C}^{g_\alpha e_\beta}(t)$ also shows a scaling with the CGC, which leads to suppressed subradiance or superradiance effects for $\alpha = -1/2$ [47]. Furthermore, the excellent agreement in Fig. 1(b) between the short-time expressions (dotted lines) and the MF dynamics (full lines) until $\Gamma t \approx 0.2$ shows that, on these time scales, the beyond-MF terms [Q in Eq. (6)] do not contribute substantially.

Further insight is provided by the *local* dipolar shift patterns $\delta_i^{g_\alpha e_\beta} \equiv 1/(2\pi t)\arctan(\langle\hat{s}_i^y\rangle/\langle\hat{s}_i^x\rangle)$ [single-particle counterpart of Eq. (4)], which directly encode the

anisotropic and geometry-dependent character of dipolar interactions. Local density shifts are amenable for experimental observation via imaging spectroscopy [27], since they are insensitive to laser drifts which are common for all atoms in the array. In Figs. 2(a)–2(d), we present the local shifts obtained with $\pi/2$ pulses on 3D lattices with $N = 10^3$ for $\alpha = -9/2$ and $-1/2$.

The magnitude of the shifts shows again an overall suppression with $|C^{e_\alpha}_{g_\alpha}|^2$, which we emphasize by rescaling the plots as $\delta_i/(\Gamma|C^{e_\alpha}_{g_\alpha}|^2 10^{-2})$. However, the dipolar patterns of the $-9/2$ and $-1/2$ transitions feature distinguishable spatial profiles: the different dispositions of maxima and minima of the local shifts go beyond the mere $|C^{e_\alpha}_{g_\alpha}|^2$ scaling.

The local shifts of the $-1/2$ transition reveal a more pronounced sensitivity to the multilevel structure compared to the $-9/2$ case, as confirmed by simulations of pure two-level atoms, which show patterns that are almost indistinguishable from the $-9/2$ case. Furthermore, a scaling with N also confirms this conclusion for the global shift, as shown in Fig. 2(e). This is because the $-1/2$ π transition has a small CGC compared to the adjacent $\sigma^{\pm}$ transitions, whereas for the $-9/2$ π transition the opposite is true, see Fig. 1(a). Therefore, nearby levels play a more important role in the $-1/2$ case.

Figure 2(f) also reveals that an appropriate choice of the geometry and laser wave vector allows one to further reduce the shift, as previously observed for two-level systems [28,31,34]. Our main finding in this regard is that the dipolar shift saturates for large N in all cases shown, except in 2D when the laser polarization is perpendicular to the atomic plane, see Figs. 3(a) and 3(b). This is because in the latter configuration, all the dipoles align perpendicular to the plane and the corresponding dipolar interactions depend only on the distance between atoms, and not on their orientation [47].

Role of magnetic fields.—Optical clock experiments are typically conducted under a bias magnetic field $\mathbf{B}$ (along the quantization axis) that allows one to spectroscopically address specific transitions. This leads to a Zeeman shift of order $\mu_0|\mathbf{B}|$ (with $\mu_0 \equiv \mu_B/\hbar$ and μ_B the Bohr magneton) for the $g_\alpha \leftrightarrow e_\alpha$ transition considered, which trivially adds to the zero-order expression of Eq. (5) and can be removed in the appropriate rotating frame. However, magnetic fields can nontrivially affect dipolar shifts at higher orders.

If the magnetic field is weak (i.e., $\mu_0|\mathbf{B}| \lesssim \Gamma$), we find the above results on the dipolar shift are only weakly affected at late times. This is because the first-order correction, Eq. (6), turns out to be independent of the magnetic field [47]. In contrast, strong magnetic fields ($\mu_0|\mathbf{B}| \gg \Gamma$) can significantly alter the short-time behavior of the shift. Large Zeeman shifts effectively suppress exchange interactions involving off-resonant transitions. In other words, $\Delta^{ij}_{g_m e_n, g_{m'} e_{n'}} = \Gamma^{ij}_{g_m e_n, g_{m'} e_{n'}} = 0$ unless

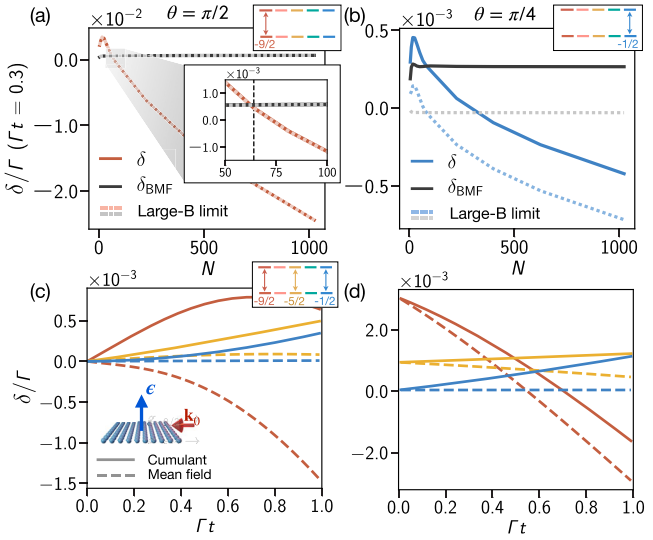

FIG. 3. Global shift for 2D arrays of atoms with laser configuration shown in (c). (a),(b) N-scaling of the total shift from the short-time expansion (red/blue) and beyond-MF contribution (black) at $\Gamma t = 0.3$: (a) $g_{-9/2} \leftrightarrow e_{-9/2}$ transition with $\pi/2$, and (b) $g_{-1/2} \leftrightarrow e_{-1/2}$ transition with $\pi/4$. The dotted, light-colored lines correspond to the large-magnetic-field limit. The inset of (a) shows the closeup region where beyond-MF corrections become comparable to the total shift. (c),(d) Dipolar shift δ as a function of the dark time: cumulant (full lines) against MF (dashed lines) approximations for the $g_{-9/2} \leftrightarrow e_{-9/2}$ (red), $g_{-5/2} \leftrightarrow e_{-5/2}$ (yellow), and $g_{-1/2} \leftrightarrow e_{-1/2}$ (blue) transitions. Simulations performed for $N = 8^2$ atoms and using (c) a $\pi/2$ and (d) $\pi/4$ pulse.

$m = m'$ and $n = n'$ (assuming different g factors for the ground and excited manifolds). This leads to an effective 4-level (or 3-level) system composed of e_α, g_α, and the ground levels adjacent to it. In this limit, almost all terms in the first-order expression, Eq. (6), involving transitions different from $g_\alpha \leftrightarrow e_\alpha$ are suppressed, except for terms with $p = p'$ appearing in $Q^{ji}_{p,p'}$ [47].

Consistently with the discussion above, we find that the modification of the shift strongly depends on the CGC of the addressed transition. For $-9/2$ neither the global nor the local shifts are substantially altered [47] [see, e.g., Figs. 2(e) and 3(a)]. In contrast, for $-1/2$ both the local shift pattern [cf. Figs. 2(b) and (c)] as well as the global shift [Figs. 2(e) and 3(b)] are significantly modified under a large $|\mathbf{B}|$. Despite this, the global shift remains suppressed by the small CGC as found for small $|\mathbf{B}|$.

Beyond-mean-field effects.—An important consequence of the strong shift suppression is that higher-order, nonclassical terms can have a contribution comparable to the lowest-order, semiclassical ones. The zero-order shift, Eq. (5), is perfectly described by the MF approach, yet the Q terms of the first-order, Eq. (6), are not. More

specifically, the difference between the shift given by the exact, first-order perturbative equations and the MF approximation reads

$$\delta_{\mathrm{BMF}}^{g_\alpha e_\beta} \equiv \frac{1}{2\pi N} \sum_{i,j\neq i} \sum_{p} \left\{ \sum_{p'} Q_{p,p'}^{ji}(\theta) - W_{\mathrm{MF},p}^{ji}(\theta) \right\}, \quad (7)$$

where $W_{\mathrm{MF},p}^{ji}(\theta)$ is a MF-only term related to W^{kji} from Eq. (6) [47]. In general, we find beyond-MF effects to be relevant in cases (but not in *every* case) where either the system is small or when a transition with small CGC is addressed.

Figure 3(c) shows the effect of beyond-MF terms for a small 8^2 lattice, driven by a $\pi/2$ pulse with a polarization orthogonal to it. There, the dynamics predicted by MF (dashed lines) substantially deviates from the cumulant result (solid lines) for all transitions considered. The relevance of the beyond-MF term in these cases lies in the comparably small magnitude of the MF part. Figure 3(a) shows that for this system size the total shift happens to be close to zero. On the contrary, at large N, when the MF contributions are no longer suppressed, the beyond-MF term becomes negligible.

Although beyond-MF corrections do not scale up with N, we find cases where they can be relevant even for large systems because of a strong suppression of the total shift by the multilevel structure. An example is the case with a pulse area of $\theta = \pi/4$ presented in Figs. 3(b) and 3(d) for the same 2D lattice configuration of (a) and (c). Because of the strong suppression of the total shift when addressing the $-1/2$ transition [see Eq. (5)], the beyond-MF contributions become comparable in magnitude to the actual shift. Figure 3(b) shows that this holds true for lattices of size up to $\sim 10^3$ atoms. Note, however, that in this case the beyond-MF term is suppressed in the large B-field limit.

Conclusion.—We have shown that dipolar frequency shifts are strongly modified in systems featuring a multilevel structure. The predicted 2 orders of magnitude suppression obtained by properly addressing specific transitions can lead to the improved accuracy necessary for the exploration of fundamental physics [21–25], providing new insights on the behavior of strongly and long-range interacting many-body systems.

We thank C. Qu, L. Sonderhouse, and N. Schine for helpful discussions and feedback. A. C. and R. B. are supported by FAPESP through Grants No. 2017/09390-7, No. 2018/18353-0, No. 2019/13143-0, and No. 2018/15554-5. R. B. benefited from grants from the National Council for Scientific and Technological Development (CNPq, Grants No. 302981/2017-9 and No. 409946/2018-4). C. S. thanks the Humboldt Foundation for support. This work is supported by the AFOSR Grant No. FA9550-18-1-0319 and its MURI Initiative, by the DARPA and ARO Grant No. W911NF-16-1-0576, the ARO single investigator Grant No. W911NF-19-1-0210, the NSF Grants No. PHY1820885, No. JILA-PFC PHY-1734006, No. QLCI-2016244, DOE-QSA, and by the NIST.

[1] T. Nicholson, S. Campbell, R. Hutson, G. Marti, B. Bloom, R. McNally, W. Zhang, M. Barrett, M. Safronova, G. Strouse, W. Tew, and J. Ye, Nat. Commun. **6**, 6896 (2015).
[2] A. D. Ludlow, M. M. Boyd, J. Ye, E. Peik, and P. O. Schmidt, Rev. Mod. Phys. **87**, 637 (2015).
[3] M. Schioppo, R. C. Brown, W. F. McGrew, N. Hinkley, R. J. Fasano, K. Beloy, T. H. Yoon, G. Milani, D. Nicolodi, J. A. Sherman, N. B. Phillips, C. W. Oates, and A. D. Ludlow, Nat. Photonics **11**, 48 (2017).
[4] R. C. Brown, N. B. Phillips, K. Beloy, W. F. McGrew, M. Schioppo, R. J. Fasano, G. Milani, X. Zhang, N. Hinkley, H. Leopardi, T. H. Yoon, D. Nicolodi, T. M. Fortier, and A. D. Ludlow, Phys. Rev. Lett. **119**, 253001 (2017).
[5] S. L. Campbell, R. B. Hutson, G. E. Marti, A. Goban, N. D. Oppong, R. L. McNally, L. Sonderhouse, J. M. Robinson, W. Zhang, B. J. Bloom, and J. Ye, Science **358**, 90 (2017).
[6] W. F. McGrew, X. Zhang, R. J. Fasano, S. A. Schffer, K. Beloy, D. Nicolodi, R. C. Brown, N. Hinkley, G. Milani, M. Schioppo, T. H. Yoon, and A. D. Ludlow, Nature (London) **564**, 87 (2018).
[7] E. Oelker, R. Hutson, C. Kennedy, L. Sonderhouse, T. Bothwell, A. Goban, D. Kedar, C. Sanner, J. Robinson, G. Marti *et al.*, Nat. Photonics **13**, 714 (2019).
[8] M. A. Norcia, A. W. Young, W. J. Eckner, E. Oelker, J. Ye, and A. M. Kaufman, Science **366**, 93 (2019).
[9] A. W. Young, W. J. Eckner, W. R. Milner, D. Kedar, M. A. Norcia, E. Oelker, N. Schine, J. Ye, and A. M. Kaufman, Nature (London) **588**, 408 (2020).
[10] R. Lange, N. Huntemann, J. M. Rahm, C. Sanner, H. Shao, B. Lipphardt, C. Tamm, S. Weyers, and E. Peik, Phys. Rev. Lett. **126**, 011102 (2021).
[11] A. M. Rey, A. V. Gorshkov, C. V. Kraus, M. J. Martin, M. Bishof, M. D. Swallows, X. Zhang, C. Benko, J. Ye, N. D. Lemke, and A. D. Ludlow, Ann. Phys. (Amsterdam) **340**, 311 (2014).
[12] X. Zhang, M. Bishof, S. L. Bromley, C. V. Kraus, M. S. Safronova, P. Zoller, A. M. Rey, and J. Ye, Science **345**, 1467 (2014).
[13] F. Scazza, C. Hofrichter, M. Höfer, P. C. D. Groot, I. Bloch, and S. Fölling, Nat. Phys. **10**, 779 (2014).
[14] L. F. Livi, G. Cappellini, M. Diem, L. Franchi, C. Clivati, M. Frittelli, F. Levi, D. Calonico, J. Catani, M. Inguscio, and L. Fallani, Phys. Rev. Lett. **117**, 220401 (2016).
[15] C. Hofrichter, L. Riegger, F. Scazza, M. Höfer, D. R. Fernandes, I. Bloch, and S. Fölling, Phys. Rev. X **6**, 021030 (2016).
[16] M. Kanász-Nagy, Y. Ashida, T. Shi, C. P. Moca, T. N. Ikeda, S. Fölling, J. I. Cirac, G. Zaránd, and E. A. Demler, Phys. Rev. B **97**, 155156 (2018).

[17] A. Goban, R. B. Hutson, G. E. Marti, S. L. Campbell, M. A. Perlin, P. S. Julienne, J. P. DIncao, A. M. Rey, and J. Ye, Nature (London) **563**, 369 (2018).
[18] L. Sonderhouse, C. Sanner, R. B. Hutson, A. Goban, T. Bilitewski, L. Yan, W. R. Milner, A. M. Rey, and J. Ye, Nat. Phys. **16**, 1216 (2020).
[19] F. Schäfer, T. Fukuhara, S. Sugawa, Y. Takasu, and Y. Takahashi, Nat. Rev. Phys. **2**, 411 (2020).
[20] A. Heinz, A. J. Park, N. Šantić, J. Trautmann, S. G. Porsev, M. S. Safronova, I. Bloch, and S. Blatt, Phys. Rev. Lett. **124**, 203201 (2020).
[21] C. W. Chou, D. B. Hume, T. Rosenband, and D. J. Wineland, Science **329**, 1630 (2010).
[22] J. Grotti *et al.*, Nat. Phys. **14**, 437 (2018).
[23] C. Sanner, N. Huntemann, R. Lange, C. Tamm, E. Peik, M. S. Safronova, and S. G. Porsev, Nature (London) **567**, 204 (2019).
[24] A. Derevianko and M. Pospelov, Nat. Phys. **10**, 933 (2014).
[25] C. J. Kennedy, E. Oelker, J. M. Robinson, T. Bothwell, D. Kedar, W. R. Milner, G. E. Marti, A. Derevianko, and J. Ye, Phys. Rev. Lett. **125**, 201302 (2020).
[26] T. Bothwell, D. Kedar, E. Oelker, J. M. Robinson, S. L. Bromley, W. L. Tew, J. Ye, and C. J. Kennedy, Metrologia **56**, 065004 (2019).
[27] G. E. Marti, R. B. Hutson, A. Goban, S. L. Campbell, N. Poli, and J. Ye, Phys. Rev. Lett. **120**, 103201 (2018).
[28] D. E. Chang, J. Ye, and M. D. Lukin, Phys. Rev. A **69**, 023810 (2004).
[29] L. Ostermann, H. Zoubi, and H. Ritsch, Opt. Express **20**, 29634 (2012).
[30] L. Ostermann, H. Ritsch, and C. Genes, Phys. Rev. Lett. **111**, 123601 (2013).
[31] S. Krämer, L. Ostermann, and H. Ritsch, Europhys. Lett. **114**, 14003 (2016).
[32] L. Henriet, J. S. Douglas, D. E. Chang, and A. Albrecht, Phys. Rev. A **99**, 023802 (2019).
[33] C. Qu and A. M. Rey, Phys. Rev. A **100**, 041602(R) (2019).
[34] G. Liu, Y. Huang, Z. Cheng, Z. Chen, and Z. Yu, Phys. Rev. A **101**, 012504 (2020).
[35] M. Hebenstreit, B. Kraus, L. Ostermann, and H. Ritsch, Phys. Rev. Lett. **118**, 143602 (2017).
[36] E. Munro, A. Asenjo-Garcia, Y. Lin, L. C. Kwek, C. A. Regal, and D. E. Chang, Phys. Rev. A **98**, 033815 (2018).
[37] A. Asenjo-Garcia, H. Kimble, and D. E. Chang, Proc. Natl. Acad. Sci. U.S.A. **116**, 25503 (2019).
[38] A. P. Orioli and A. M. Rey, Phys. Rev. Lett. **123**, 223601 (2019).
[39] A. P. Orioli and A. M. Rey, Phys. Rev. A **101**, 043816 (2020).
[40] A. V. Gorshkov, M. Hermele, V. Gurarie, C. Xu, P. S. Julienne, J. Ye, P. Zoller, E. Demler, M. D. Lukin, and A. M. Rey, Nat. Phys. **6**, 289 (2010).
[41] A. J. Daley, Quantum Inf. Process. **10**, 865 (2011).
[42] E. Kiktenko, A. Fedorov, A. Strakhov, and V. Man'ko, Phys. Lett. A **379**, 1409 (2015).
[43] C. Godfrin, R. Ballou, E. Bonet, M. Ruben, S. Klyatskaya, W. Wernsdorfer, and F. Balestro, npj Quantum Inf. **4**, 53 (2018).
[44] R. H. Lehmberg, Phys. Rev. A **2**, 883 (1970).
[45] M. Gross and S. Haroche, Phys. Rep. **93**, 301 (1982).
[46] D. F. V. James, Phys. Rev. A **47**, 1336 (1993).
[47] See Supplemental Material at http://link.aps.org/supplemental/10.1103/PhysRevLett.127.013401 for details on the equations of motion, short-time expansion, and Ramsey fringes contrast; a comparison of local shifts for two-level and multilevel systems; a discussion on the role of nonadjacent levels; and a scaling analysis of the dipolar shift with the system size N.
[48] S. Okaba, T. Takano, F. Benabid, T. Bradley, L. Vincetti, Z. Maizelis, V. Yampolskii, F. Nori, and H. Katori, Nat. Commun. **5**, 4096 (2014).